Pergamon

Int. J. Solids Structures Vol. 35, Nos 31–32, pp. 4077–4089, 1998

0020–7683/98 $19.00 + .00

PII: S0020–7683(97)00302–8

CLOSURE OF A THROUGH CRACK IN A PLATE UNDER BENDING

J. P. DEMPSEY,* I. I. SHEKHTMAN
Department of Civil and Environmental Engineering, Clarkson University, Potsdam, NY 13699-5710, U.S.A.

and

L. I. SLEPYAN
Department of Solid Mechanics, Materials and Structures, Tel Aviv University, Ramat Aviv 69978, Tel Aviv, Israel

(*Received* 18 *April* 1997; *accepted* 15 *June* 1997)

Abstract—A plate with a pre-existent through crack is considered under the action of a remote bending moment and a remote in-plane force. The problem statement is reduced to the solution of two coupled integral equations with strongly singular kernels. The independent variables in the latter equations are the closure displacement and rotation angle. The corresponding closure force and moment distributions, and the contact-crack opening boundary (the closure perimeter), are found as functions of the remote bending–compression ratio. The validity of previously stated analytical asymptotics for the contact boundary is examined. The dependence of the extent of closure on the crack length-to-thickness ratio is studied. Comparisons are made with experimental results. © 1998 Elsevier Science Ltd. All rights reserved.

INTRODUCTION

Difficulties caused by the closure of a through crack in a thin plate under bending have long been recognized (Smith, 1969; Wynn and Smith, 1969; Smith and Smith, 1970; Jones and Swedlow, 1975; Heming, 1980; Alwar and Ramachandran Nambissan, 1983). The mechanics of crack closure has received an increased scrutiny in recent years (Joseph and Erdogan, 1989; Young and Sun, 1992, 1993; Cordes and Joseph, 1995; Kuo *et al.*, 1995; Dempsey *et al.*, 1995a; Slepyan *et al.*, 1995). In particular, Joseph and Erdogan (1989) provided a plot of the closure width distribution for the case of a through-cracked plate subjected to pure bending. Slepyan *et al.* (1995) provided an analytical asymptotic solution to the latter problem valid for long cracks. The material presented therein can be considered to pose an inverse surface crack treatment to that given much earlier by Rice and Levy (1972). The present paper examines the dependencies of the shape and extent of closure on the remote loading and crack length to plate thickness ratio. The formulation provided by Slepyan *et al.* (1995) is adapted and extended. The title problem reduces to the solution of two hypersingular integral equations that yield the averaged crack opening displacement and crack face rotation. The latter quantities are coupled through the smooth closure condition along the crack front. Given that the shape of the closure region is unknown at the outset, the solution procedure is necessarily iterative. At each iteration, the solution of the integral equations follows the procedure standardized by Kaya and Erdogan (1987).

Consider a cracked infinite elastic plate $-\infty < X < +\infty$, $-\infty < Y < +\infty$ (Fig. 1) of uniform thickness $2h$, $|Z| \leqslant h$. The through-the-thickness crack of length $2l$ lies at $Y = 0$, $|X| \leqslant l$, $|Z| \leqslant h$. The plate is subjected to the action of a self-equilibrated system of the external forces. All the external loads are sufficiently remote with respect to the crack area for their action can be explicitly described by the distribution of the initial extensional inplane force $S^0(X)$ and bending moment $M^0(X)$ acting in the intact plate at $Y = 0$, $|X| \leqslant l$.

*Author to whom correspondence should be addressed. Tel.: 00 315 268 6517. Fax: 00 315 268 7985. E-mail: john@sun.soe.clarkson.edu.

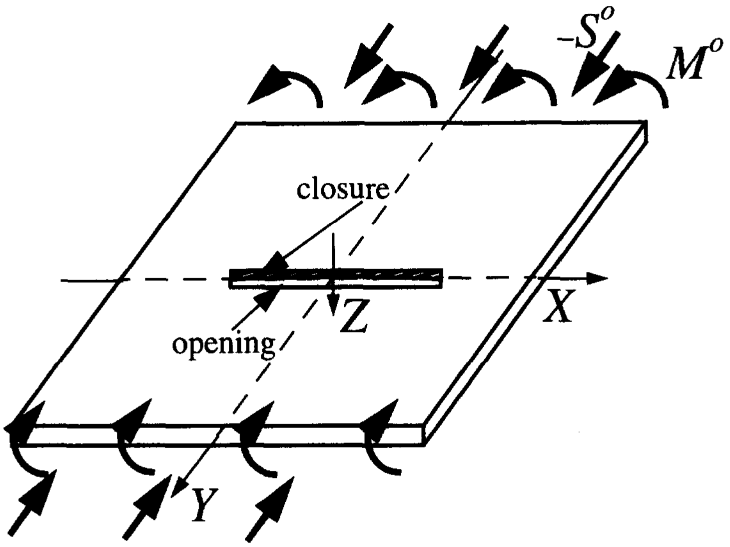

Fig. 1. A through-the-thickness crack in a plate under bending and compression.

During the imposed deformation, the two sides of the crack come into the contact with the local closure force S and bending moment M depending on X in the range $|X| \leqslant l$. The shear force within the contact region is assumed to be zero. The distribution of the local closure forces $S(X)$ and $M(X)$ and the contact area are to be determined.

The problem can be considered as the superposition of three sub-problems. The first is a plane problem (the X, Y-plane) with a through-the-thickness crack (Fig. 2(a)) under action of an inplane force, $S(X)$. The second is a bending problem for a Kirchhoff–Poisson plate containing the same crack (Fig. 2(b)) with a contact-induced bending moment, $M(X)$. The third problem is for an elastic layer containing a part-through surface crack (Fig. 2(c)) with a contact induced closure stress distribution $\Sigma(X, Z)$ acting on the region under closure, $-h \leqslant Z \leqslant h-a$, where $b(X) = 2h-a(X)$ is the closure width.

The paper by Slepyan *et al.* (1995) provides a thorough exposition of the integral equation formulation to the above superposition scenario. In the following, note that the closure-induced crack surface interaction force and moment $S(X)$ and $M(X)$ are defined in terms of the stress distribution in the closure strip

$$S(X) = \int_{-h}^{h} \Sigma(X, Z)\, \mathrm{d}Z, \quad M(X) = \int_{-h}^{h} Z\Sigma(X, Z)\, \mathrm{d}Z \tag{1}$$

and that $v(X)$ and $\phi(X)$ are the additional displacement and rotation of one end of the strip (Fig. 2(c)) relative to the other due to the crack opening displacements. On the other hand, $v(X)$ and $\phi(X)$ can be defined in terms of the closure contact problem,

$$v(X) = \frac{1}{2h}\int_{-h}^{h} \hat{v}(X, 0^+, Z)\, \mathrm{d}Z, \quad \phi(X) = -\frac{3}{2h^3}\int_{-h}^{h} Z\hat{v}(X, 0^+, Z)\, \mathrm{d}Z \tag{2}$$

where $2\hat{v}(X, 0^+, Z)$ is the crack opening displacement, and $\Sigma(X, Z)$ is the stress distribution in the closure strip.

The governing integral equations,

$$\frac{Eh}{\pi}\int_{-l}^{l} \frac{v(\xi)}{(\xi - X)^2}\, \mathrm{d}\xi = -S^0(X) + S(X)$$

$$\frac{Eh^2}{\varrho\pi}\int_{-l}^{l} \frac{\phi(\xi)}{(\xi - X)^2}\, \mathrm{d}\xi = \frac{3}{h}M^0(X) - \frac{3}{h}M(X) \tag{3}$$

associated contact equations,

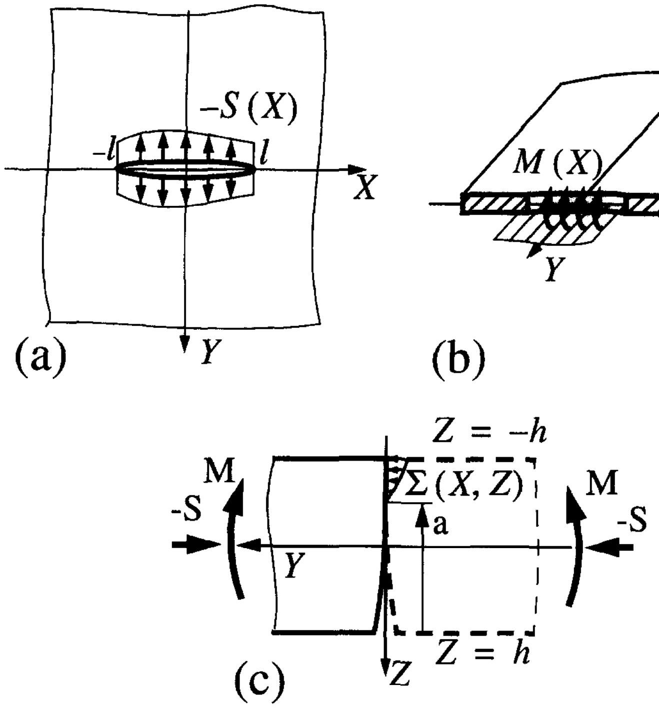

Fig. 2. Sub-problems: plane with a through crack under the action of a distributed (a) in-plane force and (b) bending moment; (c) edge-cracked strip subjected to extension and bending with closure.

$$v(X) = \frac{1}{E'}\left\{\alpha_{ss}(\zeta)S(X) + \frac{3}{h}\alpha_{sm}(\zeta)M(X)\right\}$$

$$\phi(X) = -\frac{3}{E'h}\left\{\alpha_{ms}(\zeta)S(X) + \frac{3}{h}\alpha_{mm}(\zeta)M(X)\right\} \quad (4)$$

and stress intensity factor,

$$K(a) = \frac{1}{\sqrt{2h}}\frac{\sqrt{\pi\zeta}}{(1-\zeta)^{3/2}}\left\{F_s(\zeta)S(X) + \frac{3}{h}F_m(\zeta)M(X)\right\} \quad (5)$$

are stated here without derivation. The full details are given in the paper by Slepyan *et al.* (1995). In the above equations, $\varrho = (1+\nu)/(3+\nu)$ and $E' = E/(1-\nu^2)$, while (Dempsey *et al.*, 1995b; Slepyan *et al.*, 1995)

$$\alpha_{\lambda\mu}(\zeta) = \frac{\pi\zeta^2}{(1-\zeta)^2}\Lambda_{\lambda\mu}(\zeta), \quad \zeta(X) = \frac{a(X)}{2h} \quad (6)$$

$$\Lambda_{\lambda\mu} = \sum_{i=0}^{7}\beta_i^{\lambda\mu}\zeta^i, \quad \lambda, \mu = s, m \quad (7)$$

$$F_s(\zeta) = \sum_{i=0}^{7}\alpha_i^s\zeta^i, \quad F_m(\zeta) = \sum_{i=0}^{7}\alpha_i^m\zeta^i \quad (8)$$

The coefficients $\beta_i^{\lambda\mu}$ and α_i^μ ($i = 0, 1, \ldots, 7$) in eqns (7) and (8), respectively, are provided in Slepyan *et al.* (1995). The kernel $(\xi - X)^{-2}$ can be considered as the generalized limit of

$\Re\Omega^{-2}$, $\Omega = \xi - X + iY$ when $Y \to 0$. Every Y, Z section of the plate has the shape of an edge-cracked strip as in Fig. 2(c). Under the assumptions of the line spring model (Rice and Levy, 1972), the deformation of each segment, $X = X_0$, $-h < Z < h$, is derived using the solution of the plane contact problem. This procedure is acceptable as long as the ratio of the length of the crack to the thickness of the plate $l/2h$ is sufficiently large.

The normalized extent of closure is defined by

$$\mho(X) = \frac{b(X)}{2h} = \frac{2h - a(X)}{2h} = 1 - \zeta(X) \tag{9}$$

The shape of the contact area, $\mho(X)$, or rather the shape of the open portion of the through-the-thickness crack, $\zeta(X)$, has yet to be determined. Given that the crack length $a(X)$ naturally seeks its own length under the unilateral closure conditions such that the crack surfaces end in smooth tangential contact at the crack tip, the transition from closure to contact is found by specifying that the crack-tip stress-intensity-factor in eqn (5) be zero. That is,

$$K(a) = 0 \quad \text{for } |X| < l \tag{10}$$

The condition of unilateral contact is

$$S \leqslant 0 \tag{11}$$

CLOSURE OF A THROUGH CRACK

The inversion of the expressions in eqn (4) gives

$$S(X) = \frac{E'}{\mathscr{D}} \left\{ \alpha_{mm}(\zeta) v(X) + \frac{h}{3} \alpha_{sm}(\zeta) \phi(X) \right\}$$

$$(3/h) M(X) = -\frac{E'}{\mathscr{D}} \left\{ \alpha_{ms}(\zeta) v(X) + \frac{h}{3} \alpha_{ss}(\zeta) \phi(X) \right\} \tag{12}$$

where

$$\mathscr{D} = \alpha_{ss}\alpha_{mm} - \alpha_{sm}\alpha_{ms} \tag{13}$$

By substituting the expressions in eqn (12) into eqn (5), the condition in eqn (10) becomes

$$\frac{v(X)}{h\mathscr{D}_v(X)} = \frac{\phi(X)}{2\mathscr{D}_\phi(X)} \tag{14}$$

in which

$$\mathscr{D}_v = F_s\alpha_{sm} - F_m\alpha_{ss}, \quad \mathscr{D}_\phi = F_m\alpha_{ms} - F_s\alpha_{mm} \tag{15}$$

The latter equation, in turn, simplifies the expressions in eqn (12) as follows:

$$S(X) = -\frac{E'F_m}{\mathscr{D}_v} v(X), \quad \frac{3}{h} M(X) = \frac{h}{3} \frac{E'F_s}{\mathscr{D}_\phi} \phi(X) \tag{16}$$

The integral equations in (3) may now be expressed in uncoupled form as

$$\frac{Eh}{\pi}\int_{-l}^{l}\frac{v(\xi)}{(\xi-X)^2}\mathrm{d}\xi+\frac{E'F_m}{\mathscr{D}_v}v(X) = -S^0(X)$$

$$\frac{Eh^2}{\varrho\pi}\int_{-l}^{l}\frac{\phi(\xi)}{(\xi-X)^2}\mathrm{d}\xi+\frac{h}{3}\frac{E'F_s}{\mathscr{D}_\phi}\phi(X) = \frac{3}{h}M^0(X) \tag{17}$$

For the cases studied numerically in this paper, the plate is considered under the action of a uniform and remote extensional force per unit length S^0 and a bending moment M^0 (Fig. 1). It corresponds to the uniform distribution of the initial forces in the intact plane: $S^0(X) \equiv S^0$ and $M^0(X) \equiv M^0$. The latter equations may then be simplified by introducing the following normalized variables

$$x = X/l,\quad t = \xi/l,\quad \hat{v}(x) = Ev(X)/S^0,\quad \hat{\phi}(x) = Eh\phi(X)/3S^0 \tag{18}$$

The equations in (17) now take the form

$$\frac{1}{\pi}\int_{-1}^{1}\frac{\hat{v}(t)}{(t-x)^2}\mathrm{d}t+\frac{l}{h}\frac{F_m}{\mathscr{D}_v(1-v^2)}\hat{v}(x) = -\frac{l}{h}$$

$$\frac{1}{\pi}\int_{-1}^{1}\frac{\hat{\phi}(t)}{(t-x)^2}\mathrm{d}t+\frac{\varrho l}{3h}\frac{F_s}{\mathscr{D}_\phi(1-v^2)}\hat{\phi}(x) = -\varrho\frac{l}{h}l_f^0 \tag{19}$$

where

$$l_f^0 = -\frac{M^0}{hS^0} \tag{20}$$

The above normalization with respect to the inplane force eqn (18), containing S_0 in the denominator, does not cover the case of pure bending ($S^0 = 0$) and also becomes difficult to handle numerically when $S^0 \to 0$; in this case, it is preferable to choose

$$\hat{v}(x) = Ehv(X)/M^0,\quad \hat{\phi}(x) = Eh^2\phi(X)/3M^0 \tag{21}$$

whereupon the equations in (17) take the form

$$\frac{1}{\pi}\int_{-1}^{1}\frac{\hat{v}(t)}{(t-x)^2}\mathrm{d}t+\frac{l}{h}\frac{F_m}{\mathscr{D}_v(1-v^2)}\hat{v}(x) = \frac{l}{h}m_f^0$$

$$\frac{1}{\pi}\int_{-1}^{1}\frac{\hat{\phi}(t)}{(t-x)^2}\mathrm{d}t+\frac{\varrho l}{3h}\frac{F_s}{\mathscr{D}_\phi(1-v^2)}\hat{\phi}(x) = \varrho\frac{l}{h} \tag{22}$$

where

$$m_f^0 = -\frac{hS^0}{M^0} \tag{23}$$

Note here that the case of both S^0 and M^0 tending to zero at the same time is not defined for this problem formulation unless either the ratio $l_f^0(m_f^0)$ is specified. An important additional feature, characteristic of receding contact problems, is that the extent of closure is influenced by the ratio of the initial in-plane vs out-of-plane loads, not by the individual intensities. For either normalization, the expression in (14) is now given by

$$\frac{\hat{v}(x)}{\mathscr{D}_v(X)} = \frac{\hat{\phi}(x)}{\mathscr{D}_\phi(X)} \tag{24}$$

Clearly, the solution of the equations in (19) or (22), subject to the condition in eqn (24), requires the specification of three quantities: the crack length to plate thickness ratio l/h, the initial in-plane versus out-of-plane load ratio l_f^0, and Poisson's ratio ν. The extent of closure is uniquely defined by the specification of the above three quantities.

The strongly singular integral equations in (19) and (22) are readily solved following the procedure established by Kaya and Erdogan (1987). The unknown in-plane displacement $\hat{v}(x)$ and rotation $\hat{\phi}(x)$ are represented in the form of a truncated Chebyshev polynomials of the second kind with undetermined coefficients as follows

$$\hat{v}(x) = \sum_{j=0}^{N} v_j U_{2j}(x)\sqrt{1-x^2}$$

$$\hat{\phi}(x) = \sum_{j=0}^{N} \varphi_j U_{2j}(x)\sqrt{1-x^2} \tag{25}$$

The representation in eqn (25), in recognition of the symmetrical deformations about $x = 0$, excludes $U_n(x)$ for n odd. The unknown coefficients v_j and φ_j ($j = 0, 1, \ldots, N$) are determined separately from the equations in (19) by selecting the set of collocation points given by the zeros of $T_{2N}+1$,

$$x_i = \cos\left(\frac{2i+1}{2N+1}\frac{\pi}{2}\right) \tag{26}$$

Following from eqns (3), (18) and (25), the closure forces along the crack line may be calculated via

$$\frac{S(X)}{S^0} = -\frac{h}{l}\sum_{j=0}^{N} v_j(2j+1)U_{2j}(x)+1$$

$$\frac{M(X)}{M^0} = -\frac{h/l}{\varrho l_f^0}\sum_{j=0}^{N} \varphi_j(2j+1)U_{2j}(x)+1 \tag{27}$$

The functions $S(X)$ and $M(X)$ are accurately determined in the vicinity of the crack-tips since the collocation points eqn (26) are clustered near the crack-tips. The expressions in eqn (27) quickly give $S(\pm l)$ and $M(\pm l)$ on noting that $U_{2j}(1) = 2j+1$.

The solution procedure must proceed in a semi-inverse manner. At each iteration, a particular perimeter is chosen; the equations in (19) [or (22)] are solved, then the difference

$$\varepsilon(x) = \frac{\hat{v}(x)}{\mathscr{D}_v(X)} - \frac{\hat{\phi}(x)}{\mathscr{D}_\phi(X)} \tag{28}$$

is examined. The shape $\zeta(X)$ is readjusted at each iteration until $K(a) \simeq 0$ (to the desired accuracy) for all $|X| \leqslant l$, as required by eqn (10).

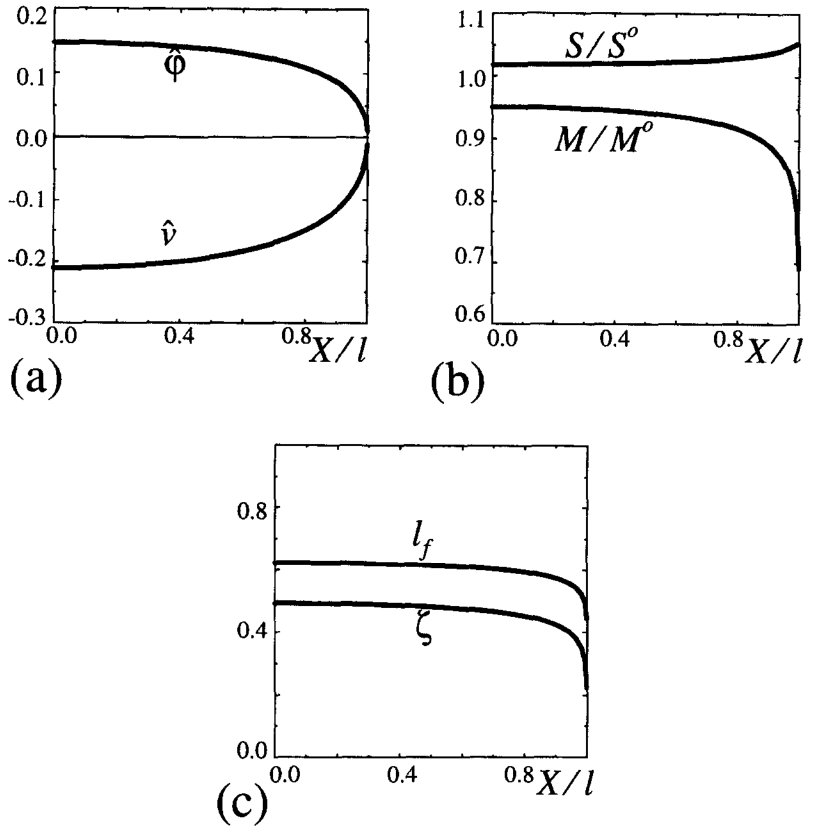

Fig. 3. Contact variable distribution versus $\hat{x} = X/l$; $l_f^0 = 2/3$, $l/h = 10$, $\nu = 0.3$: (a) normalized in-plane displacement $\hat{v}(X)$ and rotation $\hat{\varphi}(X)$; (b) the local contact induced-in-plane force $S(X)/S^0$ and bending moment $M(X)/M^0$; (c) local load ratio l_f and relative through-the-thickness length of the crack ζ.

Results obtained by solving the integral equations in (19) by the iteration procedure for the case of $l/h = 10$, $l_f^0 = 2/3$ are presented in Fig. 3. The shapes of various plots shown of the displacements (Fig. 3(a)), forces (Fig. 3(b)) and closure parameters l_f [see eqns $(29)_1$ and $(30)_1$] and ζ vs the normalized coordinate $x = X/l$ are more or less typical for the whole range of possible remote loading combinations.

LIMITING CASES AND NUMERICAL COMPARISONS

The paper by Slepyan *et al.* (1995) discussed limiting cases and asymptotic solutions for the long cracks (relative to the plate depth). Three possible scenarios have been outlined identifying the influence of the remote load ratio l_f^0.

The first case relates to the case of the load in the range $0 \leqslant l_f^0 \leqslant 1/3$. In this case there is no crack opening, the sides of the crack stay in full contact, and the behavior of the plate is identical to the behavior of an intact one.

The second case concerns the range $1/3 \leqslant l_f^0 \leqslant 1$ and is associated with the solution of the plane problem for the through cracked strip (Fig 2(c)). It means that, in the central area of a sufficiently long crack sufficiently remote with respect to the crack ends, the distribution of the contact forces and displacements is uniform, and the corresponding quantities can be found from the solution of the plane problem. These quantities do not depend on the length of the crack, the only requirement is that the crack should be "sufficiently long".

The third case $l_f > 1$ does not have a plane problem analogue. In the plane problem for the through-the-thickness crack in the strip (Slepyan *et al.*, 1995), no equilibrium is possible under such a load. The plate with the through-the-thickness crack of a fixed length will stay in equilibrium because of the tensile stresses on the continuation of the crack $Y = 0$, $|X| \geqslant l$, $|Z| \leqslant h$. The asymptotics of the closure forces and displacements are dependent on the length of the crack in this case. Analytical expressions for the latter asymptotics has been given by Slepyan *et al.* (1995). The validity of the latter asymptotics requires the crack to be "sufficiently long".

The definition of "sufficiently long" in the sense of the latter asymptotics has yet to be ascertained. Similarly, the behavior of the contact-closure characteristics in the general case of arbitrary length-to-the thickness ratio l/h has yet to be determined. These unknowns are to be answered in the present work by comparing the asymptotics in Slepyan *et al.* (1995) with the results of the exact numerical analysis.

The paper by Slepyan *et al.* (1995) introduced the following closure parameters:

$$l_f(X) = -\frac{M(X)}{hS(X)}, \quad l_c = -\frac{v(X)}{h\phi(X)} \tag{29}$$

The quantities l_f and l_c may be defined from eqns (5), (10), (14), (15) and $(6)_1$ in terms of the contact-closure perimeter $\zeta(X)$ as

$$l_f = \frac{F_s}{3F_m}, \quad l_c = \frac{1}{3}\frac{\Lambda_{ss} - 3l_f\Lambda_{sm}}{\Lambda_{ms} - 3l_f\Lambda_{mm}} \tag{30}$$

Remembering that $\zeta \equiv a(X)/2h$, it is important to note that $0 \leqslant \zeta \leqslant 1$ corresponds to $1/3 \leqslant l_f, l_c \leqslant 1$. Under the remote load ratio l_f^0, as the crack length increases, crack face closure occurs over a vanishingly small closure strip equal to $2h(1-\zeta)$, in which $\zeta \to 1$, ζ being a measure of the through-the-thickness open region. The global closure parameters l_f and l_c both uniformly asymptote to unity in this situation. For the case of a uniform initial in-plane force S^0 and bending moment M^0, the closure width looks as (see Sections 8 and 11 of Slepyan *et al.*, 1995)

$$\frac{b(X)}{2h} = \frac{1+3\varrho l_f^0}{3\varrho(l_f^0-1)}\frac{b^\infty(X)}{2h}, \quad \frac{b^\infty(X)}{2h} = \frac{\pi}{2}\frac{(1-v^2)\Lambda_0 k_f}{\sqrt{1-x^2}}\frac{2h}{l} \tag{31}$$

where $k_f = 0.7361$, $\Lambda_0 = 0.6289$. In the latter equation, since l_f^0 is infinite for pure bending, the general closure width $b(X)$ is expressed in terms of the expression for pure bending, viz., $b^\infty(X)/2h$. Because of the initial assumption of a vanishingly small closure width, the expression in eqn (31) is valid only for $l_f^0 > 1$ and long cracks; the definition of how large (for specific l/h values) is now investigated numerically.

Consider a through-the-thickness crack of length $2l$ in a plate of thickness $2h$ that is subjected to a remote uniform in-plane compressive force S^0 that stays constant. Assume that the uniform remote bending moment M^0, and hence l_f^0, increase monotonically from zero. The crack must be long: let $l/h = 10$; $v = 0.3$. The corresponding numerically determined opening-closure borderlines for $l_f^0 = 0.34$, 0.4, 0.5, 2/3, 0.8, 1, 2, 5, 10 and 20, respectively, are shown in Fig. 4. The borderline for $l_f^0 \leqslant 1/3$ is not shown, because in this case there is no crack opening. The upper curve for $l_f^0 = 0.34 > 1/3$ reveals that the through-the-thickness crack has just started to open, with essentially a uniform extent of almost full closure. As the remote bending–compression ratio increases, the extent of closure progressively decreases. For $l_f^0 \geqslant 10$, the extent of closure is essentially unchanging: the associated closure perimeter tends then to the asymptote that corresponds to the pure bending $l_f^0 \to \infty$ case for the given crack length–plate thickness ratio.

The validity of the closure width asymptotic expressions presented in eqn $(31)_2$ is examined via the numerical comparisons shown in Fig. 5. Evidently, good agreement is observed away from the crack-tip vicinity for $l/h \geqslant 16$; the agreement deteriorates as the relative crack length decreases (Table 1). The agreement near the crack tips is not good, as was anticipated in Slepyan *et al.* (1995).

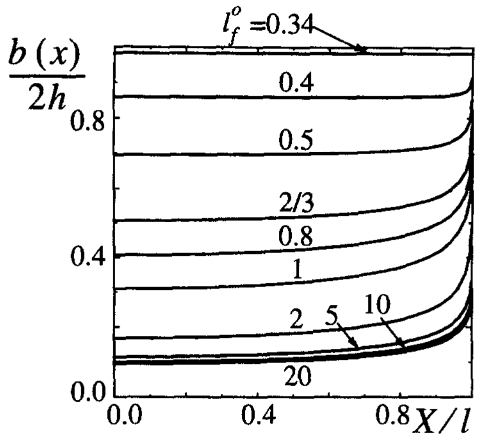

Fig. 4. Progression of the opening–closure borderline with an increasing remote load ratio ; $\nu = 0.3$, $l/h = 10$; from top to the bottom $l_f^0 = 0.34$, 0.4, 0.5, 2/3, 0.8, 1, 2, 5, 10, and 20.

Variation in the extent of closure with relative crack length l/h, given an unchanging remote load ratio $l_f^0 = 2/3$, is studied in Fig. 6(a). In connection with the discussion by Slepyan *et al.* (1995) and at the beginning of this section, $l_f^0 = 2/3$ belongs in the transitional range $1/3 \leqslant l_f^0 \leqslant 1$. If the crack is "long", in the central area the contact characteristics should coincide with those of the plane problem : $l_f \simeq l_f^0 = 2/3$, $\zeta \simeq \zeta_*$, where ζ_* is a solution of the eqn $(30)_1$ with respect to ζ for $l_f^0 = 2/3$. In particular, the latter relations should be true at the center of the crack, the point $X = 0$, which is simply the most remote with respect to the crack ends. Figure 6(a) indicates that with respect to that criterion the cracks can be considered "long" for $l/h \geqslant 8$.

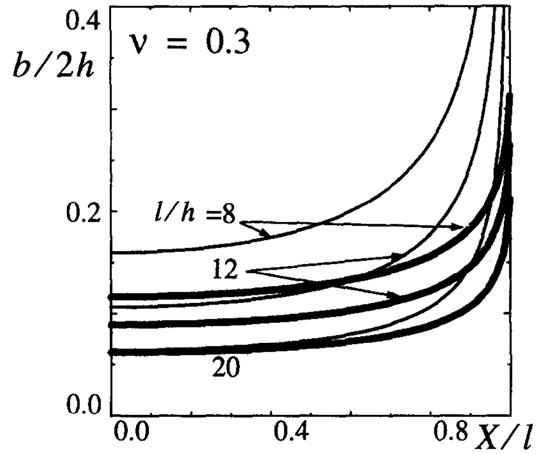

Fig. 5. Validity of the asymptotic expression in eqn $(31)_2$ for pure bending $l_f^0 \simeq \infty$. Numerical results — thick solid lines ; asymptotic expression — thin solid lines.

Table 1. Validity of the asymptotic expression in eqn $(31)_2$ for pure bending $l_f^0 \simeq \infty$: closure widths at the crack center for various l/h ratios

l/h	8	10	12	16	20
$b(0)/2h$: numerical analysis	0.117	0.101	0.0893	0.0730	0.0620
$b(0)/2h$: asymptotics eqn $(31)_2$	0.160	0.128	0.107	0.0800	0.0640
% difference	37	27	19	10	3

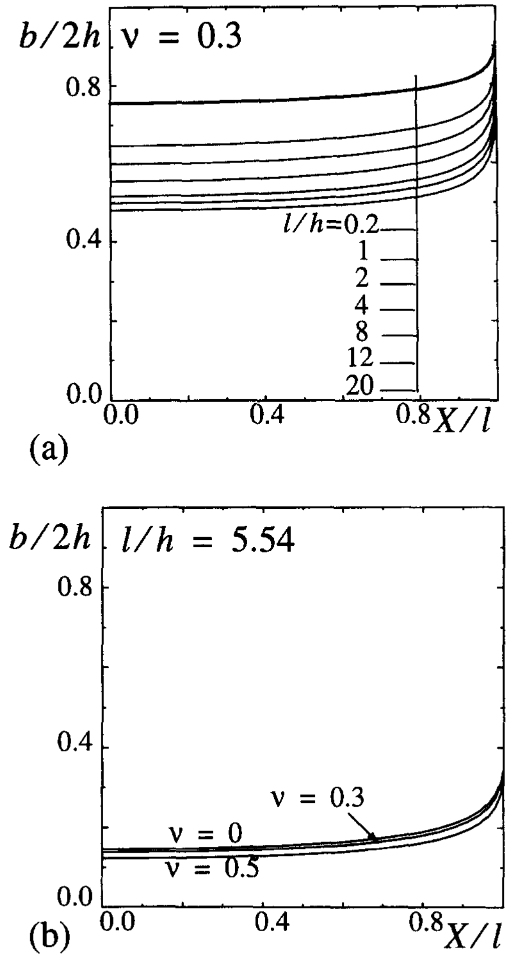

Fig. 6. Contact boundary versus the relative crack length: (a) $l_f^0 = 2/3$, various crack length to plate thickness ratio l/h; (b) influence of the Poisson ratio, pure bending $l_f^0 = \infty$.

CRACK-TIP CLOSURE CHARACTERISTICS

The shape of the opening-closure borderline in the vicinity of the crack-tip is important, especially with regard to comparisons with available experimental results (photographs of actual closures) and numerical analysis, as well the nature of crack extension. At first, one may well anticipate that $b(X) \to 2h$ as $|X| \to l$. Indeed, ahead of the crack-tip, the material is fully joined. Note that both the actual crack-line displacements and the averaged displacements $v(X)$, $\phi(X)$ are not discontinuous at the crack tip. A discontinuity in the closure perimeter $b(X)$ does not imply a discontinuous solution.

Is there a logical argument supporting a jump in the $b(X)$ as $|X| \to l \pm 0$?

Consider briefly the ramifications if the extent of closure is not discontinuous at the crack-tip. First, this implies that each crack front experiences purely compressive stresses in the vicinity of the crack tip. However, recall that the shape of the closure perimeter is governed solely by the remote load ratio $l_f^0 = M^0/h|S^0|$, and is not affected by the individual magnitudes. By this argument, there would be no load magnitude that could induce tensile stresses at the crack tip; the crack would never propagate, not for any level of the applied load. Thus, the initial assumption leads to a physical contradiction.

However, the calculations show that, under the conditions imposed by the formulation in this paper, the crack closure width $b(X)$ does not tend to the plate thickness $2h$ at the crack tip and tends to some finite value, defined here by $\beta_0 = \lim_{|X| \to l-} b(X)/2h$, $0 \leqslant \beta_0 \leqslant 1$. The β_0 values associated with the closure perimeters presented in Fig. 4 are listed in Table 2.

Table 2. Opening-contact ratio at the crack tip ($\nu = 0.3$; $l/h = 10$)

l_f^0	β_0
0.34	0.98419
0.4	0.92212
0.5	0.86410
2/3	0.79644
0.8	0.75335
1	0.69795
2	0.51165
5	0.35100
10	0.30011
20	0.27650

The observed discontinuity in the crack closure shape apparently follows directly from two assumptions, viz., the stress intensity factor is assumed to be zero in the through-the-thickness direction as $Z \to a(X)$, while the crack length $-l < X < l$ is assumed to be invariable under increasing load ratios. This profile discontinuity should disappear if the entire contact borderline were to be subject to the same fracture criterion.

COMPARISONS WITH EXPERIMENTAL RESULTS

More than two decades ago, a number of interesting photoelastic investigations of the influences of crack closure on the local bending stresses in cracked plates were completed (Smith, 1969; Wynn and Smith, 1969; Smith and Smith, 1970). The test geometry studied by Smith and coworkers is shown in Fig. 1, with the obvious exception that a finite rectangular plate was used. The material of the plate selected for the experiments was Hysol CP5-4290; for this rubber-like material (especially at higher temperatures), Poisson's ratio is well approximated by $\nu = 0.5$ (Smith and Smith, 1970). In this context, note that the extent of closure does not vary significantly with Poisson's ratio (see Fig. 6(b)).

The remote load condition in the experiment (Smith and Smith, 1970) was pure bending, $l_f^0 \simeq \infty$. Figure 7 presents closure–opening curves $b(X)$ plotted for the values of parameters that were used in the experiment (Smith and Smith, 1970). In Smith and Smith (1970), a photograph (see Fig. 8 therein) of one experiment shows the closure configuration and closure–opening border for the case $l/h = 3.58$. The highlighted curve in Fig. 7 corresponding to the latter case compares well with the closure borderline in the photograph in Smith and Smith (1970).

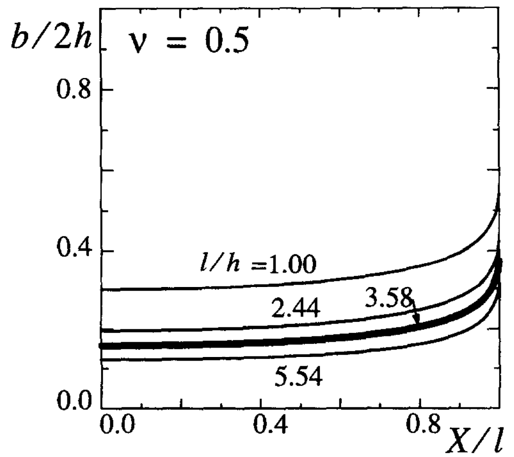

Fig. 7. Numerical closure width distributions for the tests numbered 1–4 in Smith and Smith (1970).

Table 3. Crack center closure widths

Test number	1	2	3	4
l/h	1.00	2.44	3.58	5.54
$b(0)/2h$: experiment	0.41	0.33	0.30	0.17
$b(0)/2h$: this paper	0.30	0.20	0.16	0.12
% difference	28	39	47	29

The study by Smith and Smith (1970) presents experimental measurements for the location of the minimum point $b(0)$ of the crack-closure border (see below Table 1 in the latter paper). That data is listed in this paper in Table 3 and compared with the numerical results obtained in the present work. The disagreement between the experimental vs numerical crack center closure widths is substantial and not obviously dependent on the l/h ratio. Moreover, one does not expect a higher order plate theory to alter the $b(0)/2h$ values at the crack center significantly. More plausible reasons for the noted differences in Table 3 would be a varying and non-zero in-plane compression as well as the finite size of the test specimens. The measured crack sizes should be rather reliable, as the photoelastic experiments quoted in Table 3 were not characterized by precatastrophic surficial crack extensions (D. G. Smith, 1997).

D. G. Smith (1997) noted that the contact boundary could have been determined during his thesis (not just the closure depth), as well as the distribution of the contact stress along the closed region. He also noted that the main experimental difficulty resided in making the cracks used to form the surface crack in the brittle material. The surface crack was actually created by tapping in two straight, non-twisted edge cracks into two separate plates and then joining these two edges at the edge-crack-mouths. In the frozen stress technique used, the custom was to stay away (if possible) from this glued interface (C. W. Smith, 1997). The glue on this interface contracts upon curing, and even if the residual stress caused thereby is released upon heating above the critical temperature, local residual deformations may have occurred. The $b(0)$ measurements reported in Table 3 of this paper were made precisely at the right-angled symmetrical intersection of the surface crack and the glued plane. Clearly, more experimental research on this topic is warranted.

CONCLUSIONS

The shape of the closure region and its dependence on the remote loading and crack length to plate thickness ratio has been determined for the case of a pre-existing through crack in a plate. The evolution of both the shape and extent of closure has been determined in detail for the case of an increasing applied far-field moment to in-plane force ratio given a particular crack length to plate thickness ratio. The evolution of both the shape and extent of closure has also been determined for the case of an increasing crack length to plate thickness ratio given a specific applied far-field moment to in-plane force ratio. Previously stated analytical asymptotes for the latter two cases were examined quantitatively. Comparisons were made also with experiments completed nearly three decades ago, although the experimental setup and material used to not provide the idealized comparisons desired.

Acknowledgement—This study was supported in part by the U.S. Office of Naval Research, Grant N00014-96-1-1210.

REFERENCES

Alwar, R. S. and Ramachandran Nambissan, K. N. (1983) Three-dimensional finite element analysis of cracked plates in bending. *Engineering Fracture Mechanics* **17**, 323–333.

Cordes, R. D. and Joseph, P. F. (1995) Surface and internal cracks in a residually stressed plate. *International Journal of Fracture* **68**, 287–314.

Dempsey, J. P., Slepyan, L. I. and Shekhtman, I. I. (1995a) Radial cracking with closure. *International Journal of Fracture* **73**, 233–261.

Dempsey, J. P., Adamson, R. M. and DeFranco, S. J. (1995b) Fracture analysis of base-edge-cracked reverse-tapered plates. *International Journal of Fracture* **69**, 281–294.

Heming, F. S. (1980) Sixth order analysis of crack closure in bending of an elastic plate. *International Journal of Fracture* **16**, 289–304.

Jones, D. P. and Swedlow, J. L. (1975) The influence of crack closure and elasto-plastic flow on the bending of a cracked plate. *International Journal of Fracture* **11**, 897–914.

Joseph, P. F. and Erdogan, F. (1989) Surface crack problems in plates. *International Journal of Fracture* **41**, 105–131.

Kaya, A. C. and Erdogan, F. (1987) On the solution of integral equations with strongly singular kernels. *Quarterly of Applied Mathematics* **45**, 105–122.

Kuo, C. H., Keer, L. M. and Cordes, R. D. (1995) A note on the line spring solution for a part-through crack. *International Journal of Fracture* **72**, 191–195.

Rice, J. R. and Levy, N. (1972) The part-through surface crack in an elastic plate. *Journal of Applied Mechanics* **39**, 185–194.

Slepyan, L. I., Dempsey, J. P. and Shekhtman, I. I. (1995) Asymptotic solutions for crack closure in an elastic plate under combined extension and bending. *Journal of the Mechanics and Physics of Solids* **43**, 1727–1749.

Smith, C. W. (1997) Personal communication.

Smith, D. G. (1969) A photoelastic determination of the effect of crack closure on bending stress intensity. Ph.D. dissertation, Virginia Polytechnic Institute, Blacksburg, Virginia.

Smith, D. G. (1997) Personal communication.

Smith, D. G. and Smith, C. W. (1970) A photoelastic evaluation of the influence of closure and other effects upon the local bending stresses in cracked plates. *International Journal of Fracture Mechanics* **6**, 305–318.

Wynn, R. H. and Smith, C. W. (1969) An experimental investigation of fracture criteria for combined extension and bending. *Journal of Basic Engineering* **91**, 841–849.

Young, M. J. and Sun, C. T. (1992) Influence of crack closure on the stress intensity factor in bending plates—a classical solution. *International Journal of Fracture* **55**, 81–93.

Young, M. J. and Sun, C. T. (1993) On the strain energy release rate for a cracked plate subjected to out-of-plane bending moment. *International Journal of Fracture* **60**, 227–247.